

Ecology, Spatial Structure, and Selection Pressure Induce Strong Signatures in Phylogenetic Structure

Matthew Andres Moreno^{1,2,3,*}, Santiago Rodriguez-Papa⁴, and Emily Dolson^{4,5}

¹Department of Ecology and Evolutionary Biology, University of Michigan, Ann Arbor, United States

²Center for the Study of Complex Systems, University of Michigan, Ann Arbor, United States

³Michigan Institute for Data Science, University of Michigan, Ann Arbor, United States

⁴Department of Computer Science and Engineering, Michigan State University, East Lansing, United States

⁵Program in Ecology, Evolution, and Behavior, Michigan State University, East Lansing, United States

*corresponding author: morenoma@umich.edu

Abstract

Evolutionary dynamics are shaped by a variety of fundamental, generic drivers, including spatial structure, ecology, and selection pressure. These drivers impact the trajectory of evolution, and have been hypothesized to influence phylogenetic structure. For instance, they can help explain natural history, steer behavior of contemporary evolving populations, and influence efficacy of application-oriented evolutionary optimization. Likewise, in inquiry-oriented artificial life systems, these drivers constitute key building blocks for open-ended evolution. Here, we set out to assess (1) if spatial structure, ecology, and selection pressure leave detectable signatures in phylogenetic structure, (2) the extent, in particular, to which ecology can be detected and discerned in the presence of spatial structure, and (3) the extent to which these phylogenetic signatures generalize across evolutionary systems. To this end, we analyze phylogenies generated by manipulating spatial structure, ecology, and selection pressure within three computational models of varied scope and sophistication. We find that selection pressure, spatial structure, and ecology have characteristic effects on phylogenetic metrics, although these effects are complex and not always intuitive. Signatures have some consistency across systems when using equivalent taxonomic unit definitions (e.g., individual, genotype, species). Further, we find that sufficiently strong ecology can be detected in the presence of spatial structure. We also find that, while low-resolution phylogenetic reconstructions can bias some phylogenetic metrics, high-resolution reconstructions recapitulate them faithfully. Although our results suggest potential for evolutionary inference of spatial structure, ecology, and selection pressure through phylogenetic analysis, further methods development is needed to distinguish these drivers' phylometric signatures from each other and to appropriately normalize phylogenetic metrics. With such work, phylogenetic analysis could provide a versatile toolkit to study large-scale evolving populations.

Introduction

Within evolutionary biology, the structure of ancestry relationships among organisms within an evolving system is described as their “phylogeny.” Phylogenies detail the sequence of historical lineage-branching events that gave rise to contemporary populations. Most obviously, the phylogenetic record can reveal the ordering and timing of particular contingencies (e.g., trait originations, population separations) that gave rise to current populations (Pagel, 1999; Arbogast et al., 2002). For instance, phylogenies reconstructed from fungal gene sequences suggest frequent switching of nutritional sources and that spore-dispersal mechanisms have multiple independent origins (James et al., 2006).

However, phylogenetic analyses can also test more general hypotheses about underlying evolutionary dynamics. Rather than

seeking to detect specific events, researchers using phylogenies for this purpose instead measure structural patterns that may be indicative of different evolutionary regimes. For instance, analysis of the counts of coexisting lineages over time has been used to detect density-dependent changes in speciation rate (Rabosky & Lovette, 2008), which can be interpreted as an indication of transition away from niche expansion due to lessening availability of ecological opportunity.

Indeed, methods to infer underlying evolutionary dynamics from phylogenetic structure are increasingly harnessed for tangible, impactful applications. In evolutionary oncology, for example, phylogenetic analysis has been used to quantify patterns of tumor evolution (Scott et al., 2020; Lewinsohn et al., 2023). Likewise, pathogen phylogenies have been studied to identify dynamics of epidemiological spread of Ebola and HIV (Giardina et al., 2017; Saulnier et al., 2017; Voznica et al., 2022). Phylogenetic information also has a long history of helping identify policy priorities for ecological conservation (Forest et al., 2007).

In computational evolutionary systems, phylogenetic structure metrics are a powerful tool for summarizing evolutionary history (Dolson et al., 2020). These analyses can help digital systems further our knowledge of biology, but they are also directly valuable for learning about digital systems themselves. Notably, within the realm of artificial life research, phylogeny-based metrics have been proposed to identify hallmarks of open-ended evolution (Dolson et al., 2019). They have also been used to understand evolutionary trajectories that lead to outcomes of interest (Lenski et al., 2003; Lalejini & Ofria, 2016; Johnson et al., 2022). For evolution-inspired optimization algorithms, phylogeny-based metrics have been used to predict which runs of evolutionary computation will be successful (Hernandez et al., 2022; Shahbandegan et al., 2022; Ferguson & Ofria, 2023) and even proactively guide artificial selection algorithms (Lalejini et al., 2024; Burke et al., 2003).

Here, we assess the potential of phylogenetic analysis as a means to study fundamental, universal evolutionary dynamics — ecology, selection pressure, and spatial structure. Specifically, we consider the following questions,

1. Do these dynamics leave detectable signatures in phylogenetic structure?
2. If so, to what extent are these dynamics' signatures discernable from one another?
3. To what extent do the structure of these dynamics' signatures

generalize across evolutionary systems?

We use *in silico* experiments to investigate these questions, and test across two levels of taxonomic abstraction. To quantify phylogenetic structure at organism-level abstraction — meaning that phylogeny is represented at the granularity of individual parent-child relationships — we use both a minimalistic, forward-time simulation and a rich artificial life system (Ofria & Wilke, 2004). In contrast, at species-level abstraction (i.e. species trees), we used a population-level simulation designed to study origins of biodiversity (Hagen et al., 2021).

A major strength of simulation experiments for this purpose is that they provide exact ground-truth phylogenies due to their perfectly observable evolutionary history. However, for *in vivo* systems perfect phylogeny tracking is not typically possible. Although new techniques are making increasingly high-fidelity lineage tracking possible in some experiments (Nozoe et al., 2017; Woodworth et al., 2017), phylogenies are still usually estimated from naturally-occurring biosequence data. Moreover, as digital evolution systems scale, issues of data loss and centralization overhead make perfect tracking at best inefficient and at worst untenable. Thus, some systems will likely need to adopt a decentralized, reconstruction-based approach similar to biological data (Moreno et al., 2024), which can be achieved through the recently-developed “hereditary stratigraphy” methodology (Moreno et al., 2022b).

Effective use of phylogenetic metrics in scenarios where exact phylogenies are not available requires understanding of potential confounding effects from inaccuracies introduced by reconstruction. However, it is in precisely such scenarios where the new capabilities to characterize evolutionary dynamics could have the largest impact; large-scale systems can produce an intractable quantity of data, making phylometrics valuable as summary statistics of the evolutionary process (Dolson et al., 2020). In particular, methods are needed to handle large-scale artificial life systems where complete, perfect visibility is not feasible and evolution operates according to implicit, contextually-dependent fitness dynamics (Moreno & Ofria, 2022; Kojima & Ikegami, 2023). Thus, an additional goal of this paper is to quantify the magnitude and character of bias that reconstruction error introduces. In particular, we calculate phylometric metrics across range of reconstruction accuracy levels, and report the level of accuracy necessary to attain metric readings statistically indistinguishable from ground truth.

The utility of a model system for experimental evolution hinges on sufficient ability to observe and interpret underlying evolutionary dynamics. Benchtop and field-based biological models continue to benefit from ongoing methodological advances that have profoundly increased visibility into genetic, phenotypic, and phylogenetic state (Woodworth et al., 2017; Blomberg, 2011; Schneider et al., 2019). Simulation systems, in contrast, have traditionally enjoyed perfect, complete observability (Hindré et al., 2012). However, ongoing advances in parallel and distributed computing hardware have begun to strain analytical omnipotence, as increasingly vast throughput introduces challenges centralizing, storing, and analyzing data (Klasky et al., 2021). These trends, although unfolding opposite one another, exhibit intriguing convergence: computational and biological domains will provide data that is multimodal and high-resolution but also incomplete and imperfect. Such convergence establishes great potential for

productive interdisciplinary exchange.

Methods

Model Systems

To assess the generality of evolutionary dynamics’ effects on phylogenetic structure, we replicated experiments across models differing in subject and approach. We used three systems,

1. a simple agent-based model with explicitly encoded fitness values;
2. Avida, a self-replicating agent-based evolutionary platform (Ofria & Wilke, 2004); and
3. Gen3sis, a population-level macro-ecological/evolutionary model (Hagen et al., 2021).

The following introduces each model and details experiment-specific configurations.

Simple Explicit-Fitness Model

Experiments testing the relationships between evolutionary dynamics, reconstruction error, and phylogenetic structure required a model system amenable to direct, interpretable tuning of ecology, spatial structure, and selection pressure. Finally, a parsimonious and generic model system was desired so that findings would better generalize across digital evolution systems. The core of this work relies on a simple agent-based model devised to fulfill these objectives.

Genomes in the simple explicit-fitness model comprised a single floating-point value, with higher magnitude corresponding to higher fitness. Population size $32,768 (2^{15})$ was used for all experiments. Selection was performed using tournament selection with synchronous generations. Treatments’ selection pressure was controlled via tournament size. Mutation was applied after selection, with a value drawn from a unit Gaussian distribution added to all genomes. Evolutionary runs were ended after $262,144 (2^{18})$ generations. Each run required around 4 hours of compute time.

Treatments incorporating spatial structure used a simple island model. In spatially structured treatments, individuals were evenly divided among 1,024 islands and only competed in selection tournaments against sympatric population members. Islands were arranged in a one-dimensional closed ring and 1% of population members migrated to a neighboring island each generation.

Treatments incorporating ecology used a simple niche model. Population slots were split evenly between niches. Organisms were arbitrarily assigned to a niche at simulation startup and were only allowed to occupy population slots assigned to that niche. Therefore, individuals exclusively participated in selection tournaments with members of their own niche. In treatments also incorporating spatial structure, an even allotment of population slots was provided for every niche on every island. Every generation, individuals swapped niches with probability $3.0517578125 \times 10^{-8}$ (chosen so one niche swap would be expected every 1,000 generations).

For our main experiments, we defined the following “regimes” of evolutionary conditions:

- *plain*: tournament size 2 with no niching and no islands,
- *weak selection*: tournament size 1 with no niching and no islands,
- *strong selection*: tournament size 4 with no niching and no islands,

- *spatial structure*: tournament size 2 with no niching and 1,024 islands,
- *weak ecology*: tournament size 2 with 4 niches and niche swap probability increased 100×,
- *ecology*: tournament size 2 with 4 niches, and
- *rich ecology*: tournament size 2 with 8 niches.

In follow-up experiments testing ecological dynamics with a spatial background, we defined the following additional evolutionary “regimes:”

- *plain*: tournament size 2 with no niching over 1,024 islands,
- *weak ecology*: tournament size 2 with 4 niches and niche swap probability increased 100× over 1,024 islands,
- *ecology*: tournament size 2 with 4 niches over 1,024 islands, and
- *rich ecology*: tournament size 2 with 8 niches over 1,024 islands.

Finally, to foster generalizability of findings, all experiments were performed with two alternate “sensitivity” variables: evolutionary length in generations and mutation operator. We saved phylogenetic snapshots at 32,768 generation epochs. This allowed us to test shorter runs of 32,768 and 98,304 generations (through epochs 0 and 2) in addition to the full-length runs (through epoch 7). One additional mutation operator was tested to contrast the unit Gaussian distribution: the unit exponential distribution. Under this distribution, deleterious mutations are not possible and large-effect mutations are more likely.

Across all experiments, each treatment comprised 50 replicates.

Avida Model

Avida is a virtual agent-based model system used for sophisticated *in silico* evolution experiments (Ofria & Wilke, 2004). Notably, unlike the simple model described above, fitness within Avida arises implicitly from agents’ self-replication activity, in relation to other agents’ self-replication and the availability of shared exogenous resources. Within Avida, digital organisms’ genomes comprise a sequence of virtual CPU instructions. Avida conducts open-ended evaluation of each agent’s genetic program, affording the opportunity of copying itself into output memory and thereby creating an offspring agent. Replication imposes an intrinsic baseline level of copy errors (i.e., mutations), ensuring an ongoing supply of genetic variation. Because self-replicators compete for a limited quantity of population slots, Darwinian evolution ensues. This scheme induces a complex fitness landscape, which is thought to better reflect the character of biological evolution (Adami, 2006).

Under baseline conditions, Avidians compete on the basis of self-replication efficiency. However, Avida may be configured to award extra CPU cycles to agents that complete boolean logic tasks. To create the potential for multiple niches, we associated each task with a depletable resource. Avidians only receive CPU cycles for completing a task if the corresponding resource is available, and completing a task depletes the associated resource. Importantly, tasks can each be associated with different resources, or they can all be associated with the same resource. Association of each task to an independent resource creates potential for stable ecological co-existence between task-specialized clades. We added the constraint that Avidians may harvest at most two tasks with the intention of preventing generalists from disrupting task specialization.

Our baseline “*plain*” treatment rewarded four boolean logic tasks (echo, not, nand, and), all drawing from a single resource with

inflow rate 400 units per update. Population structure was well-mixed and, to somewhat weaken the fecundity of high-fitness Avidians, replication destroyed the parent organism with probability 0.2.

We surveyed six additional “regimes” of evolutionary conditions, defined according to pre-existing Avida configuration options. Notably, compared to the simple model above, these manipulations are somewhat more indirect and, therefore, potentially weaker in nature. We anticipate they might better reflect the character of variations in evolutionary drivers that might be encountered in practice.

Regimes were configured as follows,

- *weak selection*: the probability of parent death was increased to 0.5;
- *strong selection*: parent death probability was set to 0.0 and offspring were protected from replacement by their own offspring;
- *spatial structure*: population was arranged as a two-dimensional toroidal grid, with Avidians replicating exclusively between neighboring population sites;
- *weak ecology*: tasks were assigned independent resource pools, but three resources were only supplied at an inflow rate of 33 units while the fourth was supplied at 300 units per update,
- *ecology*: each task drew from an independent resource pool with inflow rate of 100 units, and
- *rich ecology*: 28 tasks were rewarded, each drawing from an independent resource pool with an inflow rate of 100 units.

In follow-up experiments, we defined the following additional evolutionary “regimes” with two-dimensional toroidal spatial structure,

- *plain*: four boolean logic tasks drawing from a single resource with inflow rate 400 units per update,
- *weak ecology*: tasks were assigned independent resource pools, but three resources were only supplied at an inflow rate of 33 units while the fourth was supplied at 300 units per update,
- *ecology*: each task drew from an independent resource pool with inflow rate of 100 units, and
- *rich ecology*: 28 tasks were rewarded, each drawing from an independent resource pool with an inflow rate of 100 units.

Experimental treatments using Avida comprised 30 replicates, conducted with population size 3,600 for durations of 100,000 time steps (c. 20k generations; range 9k-40k).

In order to achieve the phylogenetic tracking necessary for our experiments, we used a fork of Avida originally developed for research on MODES (Dolson et al., 2019), linked in supplemental materials described below. This tracking system allowed two configurations: (1) tracking on the level of individual agents, where each Avidian constituted a taxonomic unit, or (2) tracking on the level of genotypes, where clonal sets of Avidians with identical genotypes constituted a taxonomic unit. Figure 1 compares example phylogenies from Avida under the “plain” treatment, tracked at organism and genome level. Surprisingly, we noticed several sign-change differences between individual-level and genotype-level tracking with respect to treatments’ effects on phylometrics (Figures 5d and 9). Much, but not all, of the difference related to effects of spatial structure. These differences may be in part related to occurrences of polytomies within genotype-level tracked phylogenies, as arbitrarily resolving polytomies into sets of bifurcating nodes gave somewhat more similar results to individual-level track-

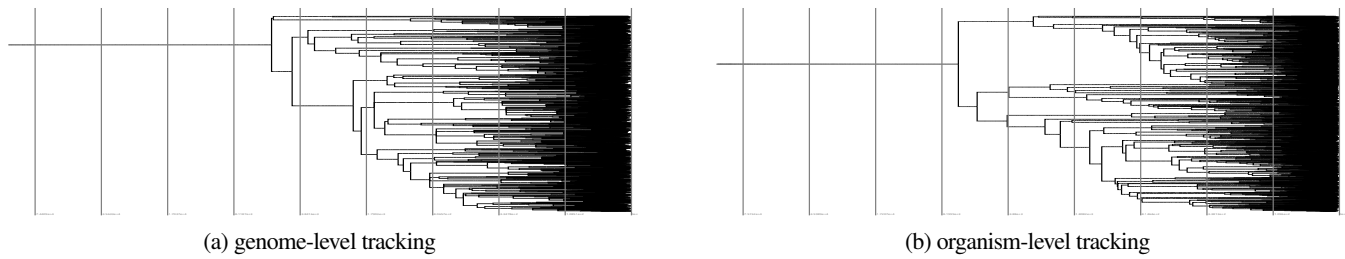


Figure 1: Sample reference phylogenies from *Avida* under “plain” regime. Time axis is log-scale.

ing. Here, we report results from individual-level tracking, which corresponds to how phylogenies were tracked in the simple model.

Gen3sis Model

In contrast to *Avida* and the simple model, which are agent-based, Gen3sis is a population-level model. Gen3sis abstracts evolution to interactions between spatially-dispersed, speciating subpopulations. Co-located subpopulations of different species compete for shares of site-specific carrying capacity. Interaction between subpopulation traits and environmental factors (e.g., aridity, temperature) mediates abundance determinations. Disjoined subpopulations of the same species accumulate genetic incompatibilities absent sufficient gene flow and, past a defined incompatibility threshold, speciate. Within this model, the taxonomic unit of phylogeny is species.

Gen3sis also stands out in its intended level of direct biological realism. The software can be configured to reflect the particular geological and climate histories of continental biomes. For our experiments, we used curated raster files depicting conditions over 30 million years in South America bundled with the package that had been synthesized from a number of sources (Straume et al., 2020; Westerhold et al., 2020; Fick & Hijmans, 2017; Hagen et al., 2019; Annan & Hargreaves, 2013; Cramwinckel et al., 2018; Evans et al., 2018; Hollis et al., 2019; Hutchinson et al., 2018; Keating-Bitonti et al., 2011; Sijp et al., 2014; Zhang et al., 2019).

Among other features, Gen3sis allows differentiation of aquatic (e.g., lakes, ocean) zones from terrestrial regions with respect to suppression of inter-population migration rates. To enhance potential for manipulable spatial structure within the model, we converted 30 randomly-selected thin linear segments spanning the map to be aquatic rather than terrestrial (i.e., “rivers”). Spatial structure was then induced by adjusting the water traversal cost function.

We assessed the following evolutionary regimes,

- *plain*: aquatic terrain imposed no additional migration penalties and population traits did not influence abundances;
- *spatial structure*: aquatic terrain imposed a migration barrier $50\times$ that of terrestrial terrain;
- *ecology*: species abundances were determined according to how close populations’ trait value matches to site temperature; and
- *ecology + spatial structure*: the $50\times$ aquatic dispersal penalty was applied, and site temperature was used to determine species’ abundances.

Figure 2 shows an example Gen3sis phylogeny from the “plain” regime.

Gen3sis treatments comprised 30 replicates. Note that, unlike other surveyed models, Gen3sis does not operate with constant “population size.” Rather, species count increased continuously

over each of the 30 simulated 1 million year time steps as a consequence of ongoing speciation. Maximum species count per spatial site was configured as 2,500 and within the entire simulation as 25,000, although neither limit was ever reached.

Full Gen3sis configuration files are linked in supplemental materials, described below. For more on Gen3sis itself, see (Hagen et al., 2021).

Hereditary Stratigraphic Annotations and Tree Reconstruction

Experiments testing the impact of phylogenetic inference error on phylometrics employ the recently-developed “hereditary stratigraphy” technique to facilitate phylogenetic inference (Moreno et al., 2022b). This technique works by attaching heritable annotations to individual digital genomes. Every generation, a new random “fingerprint” is generated and appended to the individuals’ inherited annotations. To reconstruct phylogenetic history, fingerprints from extant organisms’ annotations can be compared. Where two organisms share identical fingerprints along the record, they likely shared common ancestry. Mismatching fingerprints indicate a split in compared organisms’ ancestry. Although extensions of hereditary stratigraphy to sexual lineages are possible (Moreno, 2024a), all lineages used for experiments were asexual in nature.

Hereditary stratigraphy enables a tunable trade-off between annotation size and estimation accuracy. Fingerprints may be discarded to decrease annotation size at the cost of reduced density of reference points to test for common (or divergent) ancestry along organisms’ generational histories.

We test four levels of fingerprint retention. Each level is described as a $p\%$ “resolution” meaning that the generational distance between reference points any number of generations k back is less than $(p/100) \times k$. So, a high percentage p indicates coarse resolution and a low percentage p indicates fine resolution. In detail, at the conclusion of 262,144 generation evolutionary runs,

- at 33% resolution 68 fingerprints are retained per genome,
- at 10% resolution 170 fingerprints are retained per genome,
- at 3% resolution 435 fingerprints are retained per genome, and
- at 1% resolution 1,239 fingerprints are retained per genome.

This work uses 1 byte fingerprints, which collide with probability $1/256$. Greater space efficiency could be achieved using 1 bit fingerprints. However, this would require careful accounting for ubiquitous generation of identical fingerprints by chance and is left to future work.

Previous work with hereditary stratigraphy used UPGMA distance-based reconstruction techniques (Moreno et al., 2022a).

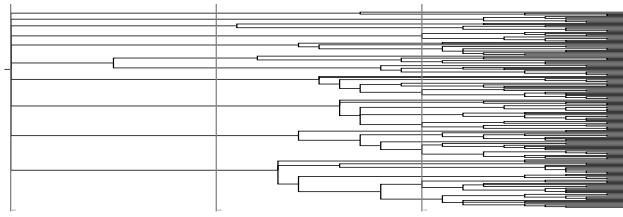


Figure 2: **Sample reference phylogeny from Gen3sis under “plain” regime.** Time axis is linear-scale.

Large-scale reconstructions required for these experiments necessitated development of a more efficient technique that did not require all pairs (i.e., $O(n^2)$) distance comparison. To accomplish this, we devised an agglomerative tree building algorithm that works by successively adding leaf organism annotations and percolating them down from the tree root along the tree path of internal nodes consistent with their fingerprint sequence, then affixing them where common ancestry ends. This new tree-building approach reduced compute time from multiple hours to around 5 minutes in most cases. Supplementary Listing ?? provides source code with full implementation details, see (Moreno et al., 2024) for a more detailed discussion.

To assess the efficacy of the new agglomerative tree-building approach, we calculated all reconstructed trees’ quartet distance to their respective reference. Quartet distance ranges from 0 (between identical trees) to 0.75 (between random trees), providing in this case a measure of reconstruction error. As expected, this measure of reconstruction error varied significantly with resolution for trees across all evolutionary regimes (Kruskal-Wallis tests; all $p < 10^{-20}$; Supplementary Table ??). Reconstruction error also varied significantly with evolutionary regime for each reconstruction resolution level (Kruskal-Wallis tests; all $p < 10^{-8}$; Supplementary Table ??).

For 3% and 1% resolutions, mean reconstruction error was less than 0.01 in all cases and at 10% resolution mean reconstruction error was less than 0.05 in all cases. At 33% resolution, mean reconstruction error was less than 0.12 in all cases. The largest reconstruction errors observed at 1%, 3%, 10%, and 33% resolutions were, respectively, 0.051 (weak selection regime), 0.093 (weak 4 niche ecology regime), 0.14 (plain evolutionary regime), and 0.45 (plain evolutionary regime). Supplementary Table ?? reports mean, median, standard deviation, and maxima for reconstruction error across surveyed evolutionary conditions.

To generate reconstructed trees in experiments, we simulated the inheritance of hereditary stratigraphic annotations along a reference phylogeny to yield the set of annotations that would be attached to extant population members at the end of a run, then used our agglomerative tree building technique to infer. Thus, each reconstruction replicate has a directly-corresponding reference tree from a perfect-tree treatment replicate. Figure 3 shows a reference tree and corresponding reconstructions performed using 1%, 3%, 10%, and 33% resolution hereditary stratigraph annotations.

Phylometrics

A wide range of metrics exists for quantifying the topology of a phylogeny. Tucker et al. showed that these metrics can

be classified into the following three dimensions: richness, divergence, and regularity (Tucker et al., 2017). Richness metrics quantify the amount of phylogenetic diversity/evolutionary history represented by a phylogeny. Divergence metrics quantify how different the units of the phylogeny are from each other. Regularity metrics quantify the variance of other properties (i.e. how consistent they are across the phylogeny). Here, we focus on four metrics spread across these categories:

Sum Pairwise Distance: This measurement sums the nodeal distance between each pair of leaf nodes. It is a metric of phylogenetic richness (Tucker et al., 2017), also referred to as F (Izsák & Papp, 2000). Consequently, we would expect it to be increased by the presence of ecology or spatial structure, as both these factors increase diversity.

Colless-like Index: The original Colless Index (Colless, 1982), also often referred to as I_c (Shao, 1990), is a measure of tree imbalance (i.e., it gets higher as the tree gets less balanced). In the context of Tucker et al.’s framework, it is a regularity metric. However, the traditional Colless Index only works for strictly bifurcating trees. As our trees have multifurcations, we instead use the Colless-like Index, which is an extension of the Colless Index to multifurcating trees (Mir et al., 2018b). Tree imbalance is thought to be associated with varying ecological pressures (Chamberlain et al., 2014; Burrell & Tan, 2017) and has also been observed to increase in the presence of spatial structure (Scott et al., 2020).

Mean Pairwise Distance: This metric is calculated by computing the shortest distance between all pairs of leaf nodes and taking the mean of these values (Webb & Losos, 2000). Note that these distances are measured in terms of the number of nodes in between the pair, not in terms of branch lengths. Mean pairwise distance is a metric of evolutionary divergence (Tucker et al., 2017). Mean pairwise distance should be increased by scenarios that promote the long-term maintenance of distinct phylogenetic branches, such as ecology. Conversely, factors that act to reduce diversity should also reduce mean pairwise distance.

Mean Evolutionary Distinctiveness: Evolutionary distinctiveness is a metric that can be calculated for individual taxa to quantify how evolutionarily different that taxon is from all other taxa in the phylogeny (Isaac et al., 2007). To get mean evolutionary distinctiveness, we average this value across all extant taxa in the tree. Like mean pairwise distance, mean evolutionary distinctiveness is a metric of evolutionary divergence. However, it is known to capture substantially different information than mean pairwise distance (Tucker et al., 2017). Unlike our other metrics, evolutionary distinctiveness is heavily influenced by branch length. We generally expect mean evolutionary distinctiveness to be

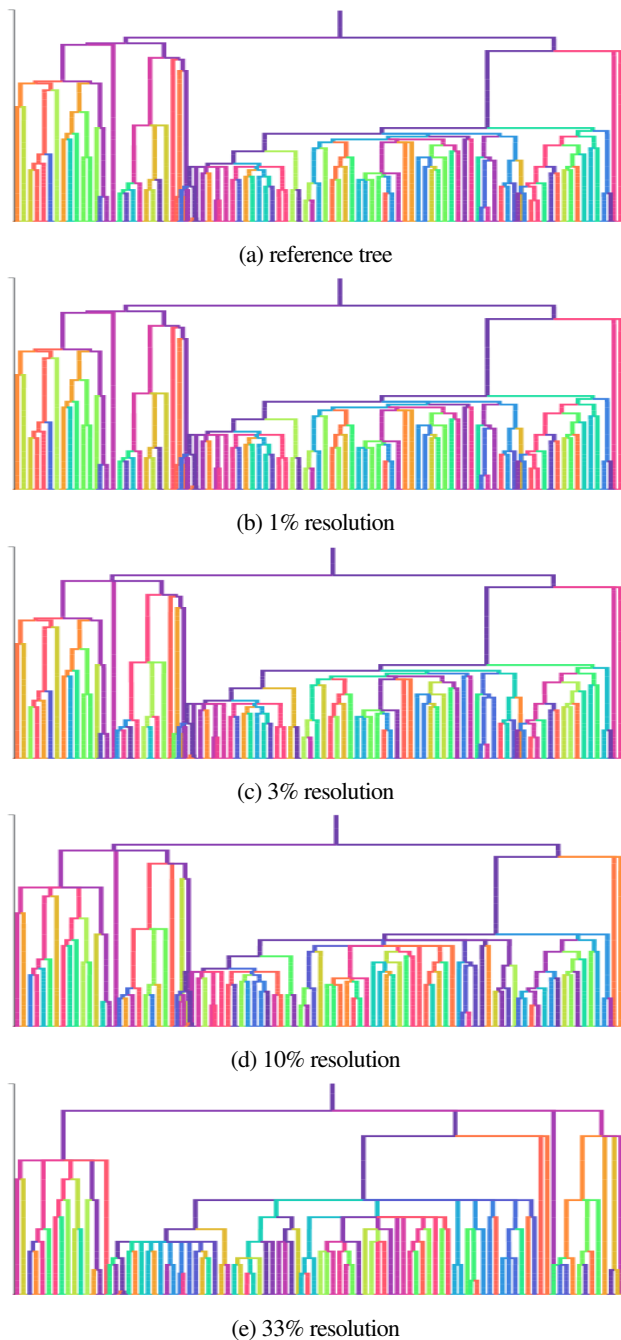


Figure 3: Comparison of phylogeny reconstructions across different hereditary stratigraphy resolutions in the plain evolutionary regime. To maintain visual legibility, these trees contain the same sub-sample of 100 leaf nodes out of the 32,768 in the full trees. Sub-figures are arranged from top to bottom in coarsening order of reconstruction resolution. Taxon and branch color coding is consistent across subpanels. Visit [mm500.com/hstrat-evolutionary-inference/](https://github.com/mm500/hstrat) for mouseover-based highlighting of corresponding clades between reconstructions and reference.

increased by similar factors to mean pairwise distance.

Effect-size Analysis

We expect statistical tests for between treatments we respect to evolutionary dynamics of interest to serve as an important use case for phylometric analyses in digital evolution. As such, we wish to report the capability of reported phylometrics to discern between surveyed evolutionary conditions.

Cliff's delta provides useful nonparametric means for such effect size analysis. This statistic reports the proportion of distributional non-overlap between two distributions, ranging from $-1/1$ if two distributions share no overlap to 0 if they overlap entirely (Kane Meissel, 2024; Cliff, 1993). When reporting effect size, we use conventional thresholds of 0.147, 0.33, and 0.474 to distinguish between negligible, small, medium, and large effect sizes (Hess & Kromrey, 2004).

Note that the Cliff's delta statistic tops/bottoms out entirely once two distributions become completely separable. Although this property suits most analyses performed, it is occasionally useful to distinguish the extent of divergence between phylometric distributions past the point of complete separability. For these purposes, we perform a simple procedure to normalize phylometrics relative baseline conditions by subtracting out the baseline mean and dividing by the baseline standard deviation.

We typically pair effect-size analysis with Mann-Whitney U testing in order to assess the extent to which differences between phylometric readings under different conditions are, or are not, evidenced by available data (Mann & Whitney, 1947). As a final detail, note that we typically report negated Cliff's delta values where necessary to ensure positive values correspond to larger phylometric values and vice versa.

Software and Data Availability

Software, configuration files, and executable notebooks for this work are available at doi.org/10.5281/zenodo.10896667. Data and supplemental materials are available via the Open Science Framework <https://osf.io/vtxwd/> (Foster & Deardorff, 2017). Note that materials for earlier versions of this work are also contained in these repositories (Moreno et al., 2023).

All hereditary stratigraph annotation, reference phylogeny generation, and phylogenetic reconstruction tools used in this work are published in the `hstrat` Python package (Moreno et al., 2022b). This project can be visited at <https://github.com/mm500/hstrat>.

This project uses data formats and tools associated with the ALife Data Standards project (Lalejini et al., 2019) and benefited from many pieces of open-source scientific software (Ofria et al., 2020; Sand et al., 2014; Virtanen et al., 2020; Harris et al., 2020; pandas development team, 2020; Wes McKinney, 2010; Sukumaran & Holder, 2010; Cock et al., 2009; Dolson et al., 2024; Torchiano, 2016; Waskom, 2021; Hunter, 2007; Moreno & Papa, 2024; Moreno, 2024b, 2023; Hagen et al., 2021; Ofria & Wilke, 2004; Torchiano, 2016).

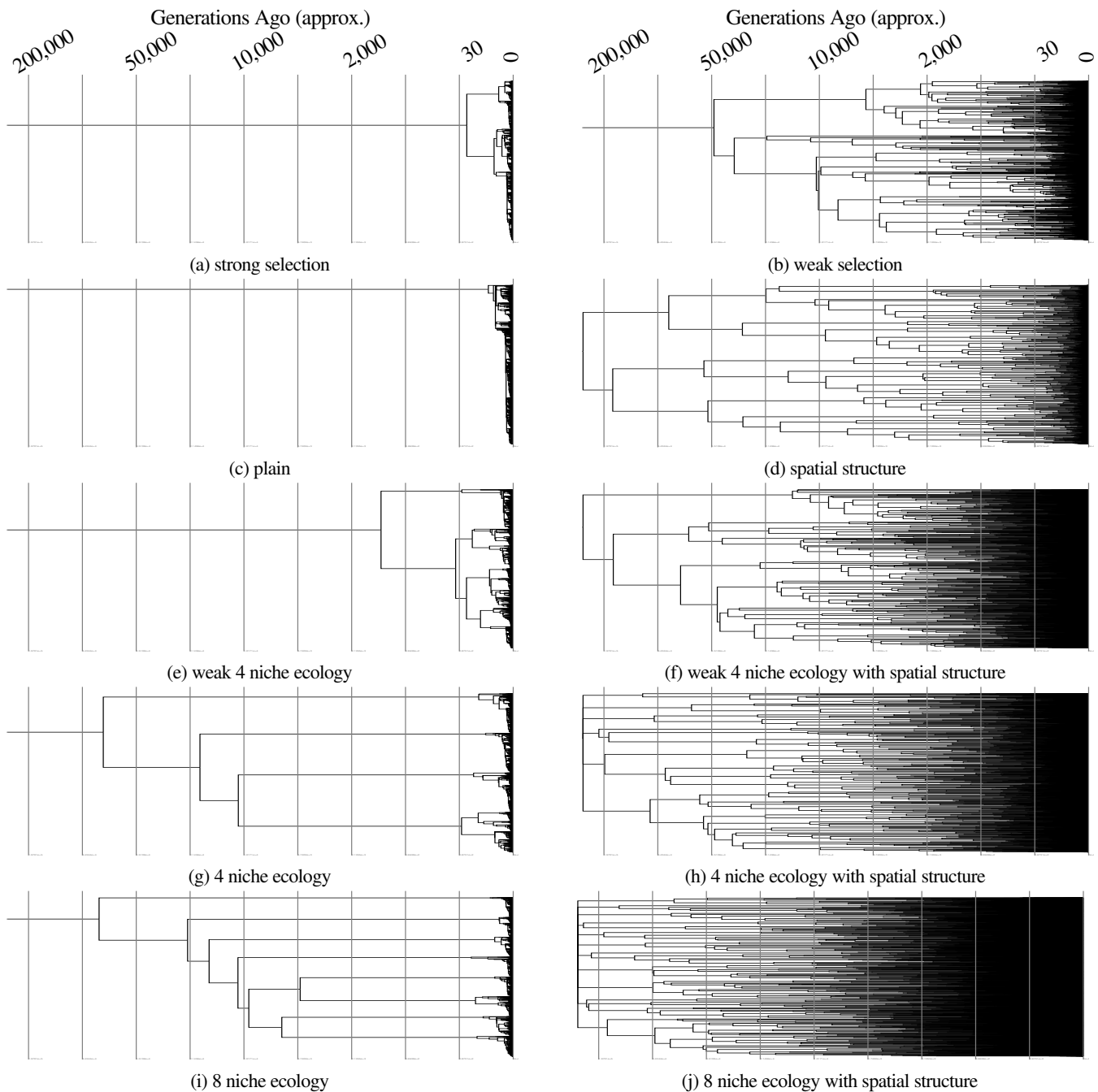


Figure 4: Sample reference phylogenies across surveyed evolutionary metrics. Each phylogeny has 32,768 leaves. Note log-scale x axis.

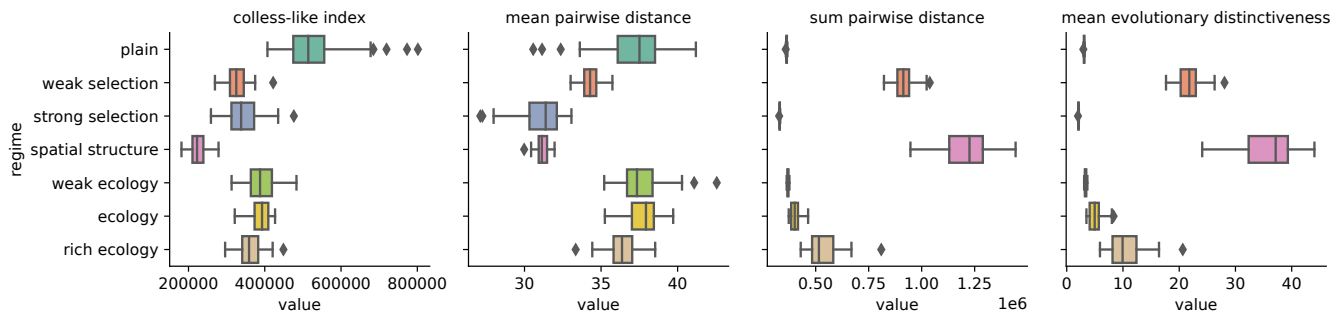
Results and Discussion

Phylometric Signatures of Evolutionary Dynamics

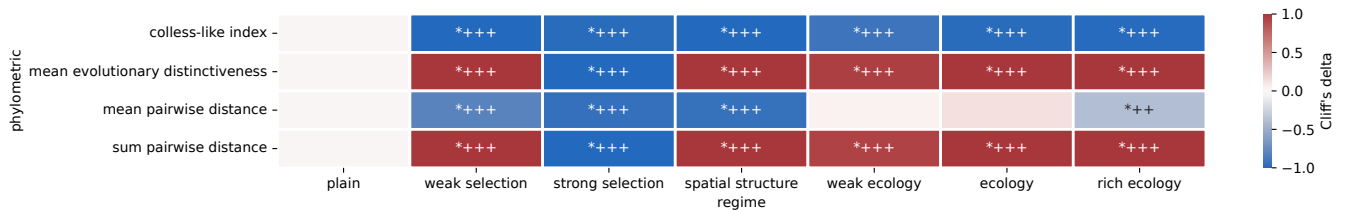
The feasibility of harnessing phylogenetic analysis to identify evolutionary dynamics hinges on the premise that these dynamics induce detectable structure within the phylogenetic record. Fortunately, as shown in Figure 4, dendrograms of phylogenetic histories from the different evolutionary conditions tested do indeed exhibit striking visual differences.

As a first step to characterizing the phylogenetic impact of spa-

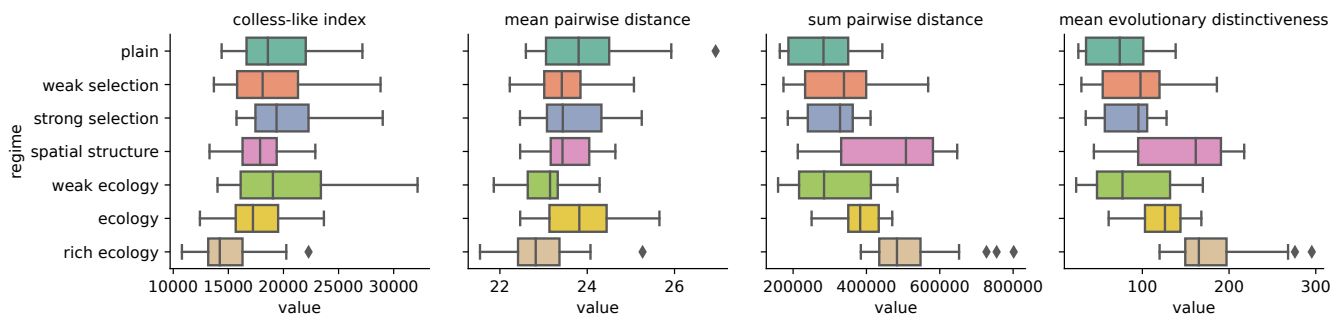
tial structure, ecology, and selection pressure, we tested whether surveyed evolutionary conditions exhibited detectable differences in a representative suite of four phylometrics: evolutionary distinctiveness, Colless-like index, mean pairwise distance, and sum pairwise distance. Figure 5 summarizes the distributions of each metric across surveyed conditions. Statistical tests confirmed that each phylometric exhibited significant variation among surveyed evolutionary conditions for both the simple model and Avida (Kruskal-Wallis tests; all $p < 10^{-40}$; $n = 50$ per condition



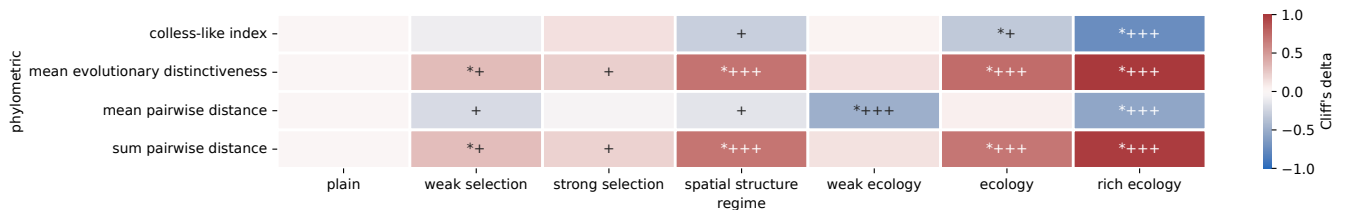
(a) Distribution of phylogenetics under the simple model. Sample sizes $n=50$.



(b) Sizes of the effect of evolutionary regimes on each phylogenetic relative to “plain” baseline in the simple model. Sample sizes $n=50$.



(c) Distribution of phylogenetics in Avida. Sample sizes $n=30$.



(d) Sizes of the effect of evolutionary regimes on each phylogenetic relative to “plain” baseline in Avida. Sample sizes $n=30$.

Figure 5: Phylogenetic responses for simple model and Avida. Phylogenetics across surveyed evolutionary regimes, calculated on perfect-fidelity individual-level phylogenies from the simple model and Avida. Note that nonparametric effect size normalization caps out to 1.0/-1.0 past the point of complete distributional nonoverlap. For heatmap charts, +’s indicate small, medium, and large effect sizes using the Cliff’s delta statistic and *’s indicate statistical significance at $\alpha=0.05$ via Mann-Whitney U test. Results from simple model are for standard experimental conditions: gaussian mutation distribution at epoch 7 (generation 262,144). See Figure ?? for results under sensitivity analysis conditions.

simple model, $n=30$ Avida; Supplementary Table ??).

To quantify the phylometric effects of surveyed evolutionary regimes, we performed nonparametric statistical comparisons against the “plain” baseline treatment. We used a measure of distributional overlap — Cliff’s delta — to assess effect sizes, binning into “negligible”, “small” (+), “medium” (++), and “large” (+++) effects based on conventional thresholds (Hess & Kromrey, 2004). Significance at $\alpha = 0.05$ (*) was assessed through Mann-Whitney tests. Figure 5b shows nonparametric significance and effect size test results.

Summary of Phylometric Effects

Relative to the plain regime, all evolutionary regimes in the simple model depress the Colless-like index. Reduction in this statistic indicates that all deviations from baseline conditions increased regularity in generated phylogenies. This observation runs somewhat counter to prior results on similar tree balance metrics, in which the presence of spatial structure increased imbalance (Scott et al., 2020). One possible contributing factor is that taxa in our phylogenies were individuals, whereas Scott et al. used genotype-level abstraction (i.e., their trees were gene trees). This possible effect of taxonomic unit is consistent with our results from the species-level phylogenies in the Gen3sis system (Figure 8), in which ecological and spatial conditions elevated Colless imbalance. Avida individual-level phylogenies were more consistent with the simple model than with Gen3sis; Colless index was significantly depressed under ecological regimes, and weakly but insignificantly depressed under spatial structure. However, other modes of evolution did not meaningfully affect Colless-like index of Avida phylogenies.

Colless-like index is sensitive to changes in evolutionary conditions. However, it appears to be the least useful metric in distinguishing different drivers of evolutionary dynamics, decreasing significantly under all non-plain evolutionary conditions.

Mean evolutionary distinctiveness was significantly higher under weak selection and with spatial structure than in the plain regime. This metric significantly decreased under strong selection and under ecological regimes, but the numerical magnitudes of these effects were relatively smaller (Figure 6). We observed similar results in Avida, except no significant effect of strong selection and weak ecology was detected on the phylometric outcome.

Mean pairwise distance was significantly depressed under all regimes except ecology and weak ecology, although again the numerical magnitude of effects on ecological regimes were relatively smaller (Figure 6). Within Avida, weak but insignificant depressing effects were observed under weak selection and spatial structure regimes. In contrast to results from the simple model, the strongest depressing effects were observed under the weak ecology and strong ecology regimes.

Finally, sum pairwise distance was significantly increased under all regimes compared to baseline, except for the strong selection regime where it was significantly depressed. Effect size was again strongest under spatial structure and weak selection (Figure 6). Avida gave similar results, except that no significant effect was detected from the weak ecology and strong selection treatments, with a weak but insignificant increase effect detected under strong selection.

Discussion of Phylometric Effects

Ecological dynamics have significant influence on the surveyed phylometrics. However, the numerical magnitudes of these effects are generally weak compared to spatial structure and selection effects (Figure 6). So, it appears careful accounting for other evolutionary dynamics (i.e., selection pressure and spatial structure) will be essential to accurate detection of ecology through phylogenetic analysis. Mean pairwise distance may play a role in identifying ecological dynamics, as ecological dynamics — in contrast to other factors such as spatial structure and changes in selection pressure — have weaker effects on this phylometric. Other phylogenetic metrics may also be better suited to detecting ecological dynamics (e.g. the ecology metric in (Dolson et al., 2019)).

Phylometric outcomes within Avida generally mirror the simple fitness model, although in many cases phylometric effects are weaker or not significant. These less pronounced effects are not unexpected — whereas the simple model was explicitly designed for direct manipulation of evolutionary drivers, we use more subtle configurations to impose evolutionary drivers on the Avida model (particularly, with respect to selection pressure). Notably, the strong selection treatment resulted in no significant effects on phylometric values. Weak selection significantly increased mean evolutionary distinctiveness and sum pairwise distance, as with the simple model, but the effect size was small. However, spatial structure’s effect size on these metrics was large and agreed with the simple model. The ecology and rich ecology treatments agreed in sign with the simple model and generally had large effect size. However, unlike the simple model, Avida’s sole phylometric outcome under weak ecology was a strong, significant decrease in mean pairwise distance. In contrast, the simple model exhibited no effect on this metric under the weak ecology treatment.

We additionally performed a sensitivity analysis for results from the simple model over an alternate exponential mutation operator and earlier phylogeny sampling time points. The effects of evolutionary conditions on phylometrics were generally consistent with Figure 5b across surveyed conditions (Supplementary Figures ???).

Phylometric Signatures of Ecological Dynamics in Spatially Structured Populations

The effects of spatial structure are of particular interest, as evolution within very large populations typically entail elements of spatial structure owing to dispersal across geographic terrain. Even within *in silico* contexts, populations too large for a single processor will almost inevitably integrate spatial structure that reflects practical limitations of distributed computing hardware (Ackley & Small, 2014; Moreno et al., 2021). Therefore, understanding the background effects of spatial structure on the phylogenetic signatures of other evolutionary dynamics will be essential to applications of phylogenetic inference in such applications. For this analysis, we chose to focus on ecological dynamics due to interest in how their relatively weak phylometric signatures would respond to the relatively strong influence of spatial structure (Figure 6).

Summary of Phylometric Effects with Background Spatial Structure

Figure 7 summarizes the distribution of surveyed phylometrics under the three surveyed ecological regimes and the control non-ecological regime, all with spatial population structure. Sta-

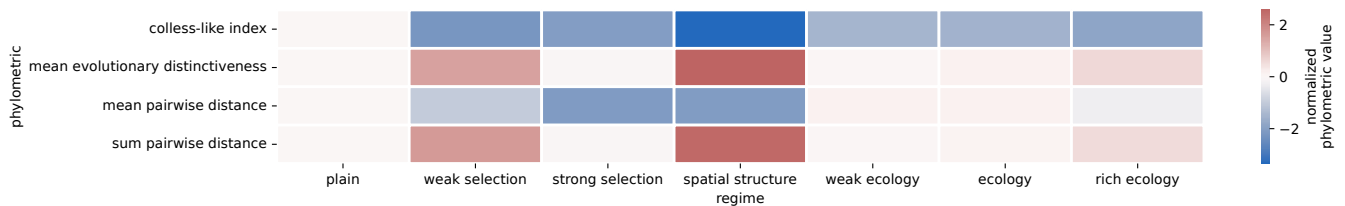


Figure 6: **Normalized phylometric responses.** Heatmap of normalized tree phylometrics across surveyed evolutionary regimes, calculated on perfect-fidelity phylogenies from the simple model. Note that normalization shows magnitude of phylometric effect beyond the point of distributional nonoverlap, unlike nonparametric normalization which tops out with complete distributional nonoverlap.

tistical tests confirmed that each phylometric exhibited significant variation among these evolutionary regimes, indicating the presence of detectable structural signatures in phylogenetic structure (Kruskal-Wallis tests; all $p < 1 \times 10^{-8}$; $n = 50$ per condition for simple model, $n = 30$ Avida; Supplementary Tables ???).

As in prior experiments, all ecology treatments drove significant increases in mean evolutionary distinctiveness and sum pairwise distance. Also consistent with spatially unstructured results, rich ecology drove significant, large-effect depression of both Colless-like index and mean pairwise distance and ecology. However, in the presence of spatial structure, the ecology treatment depressed only mean pairwise distance. Without spatial structure, the ecology treatment depressed Colless-like index instead. Results under weak ecology differed notably from non-spatial baseline, with all phylometrics seeing significant, large-effect increases. Spatial-background rich ecology results from Avida agreed with the simple model. However, significant phylometric effects were not detected from the ecology and weak ecology treatments under spatial structure conditions.

For these experiments, we again performed a sensitivity analysis over an alternate exponential mutation operator and earlier phylogeny sampling time points. We found the effects of evolutionary conditions on phylometrics to be generally consistent across surveyed conditions (Supplementary Figure ?? and Supplementary Tables ???).

Species-level Phylogenies from Gen3sis Model

Significant, large-effect changes were detected across all four phylometrics in each treatment in Gen3sis (see Figure 8). However, with the exception of sum pairwise distance, effect signs of treatments were opposite to those for individual-level phylogenies from Avida and the simple model across all phylometrics. Tip count effects seem likely to play a role in this discrepancy. Unlike Avida and the simple model, which held population size constant, species richness grew freely under the Gen3sis model. It is also possible that phylometric outcomes may be sensitive to granularity level of the taxonomic unit of the phylogeny. As noted in Section and shown in Figure 9, in Avida experiments, phylogenies using genome-level tracking (as opposed to individual-level tracking) were notably different than those using individual-level tracking. These differences also included changes in the sign of some treatment effects, lending credence to the idea that differences between Gen3sis and the individual-level phylogenies could be partially the result of Gen3sis having a more abstract taxonomic unit.

Phylometric Bias of Reconstruction Error

Shifting from perfect phylogenetic tracking to approximate phylogenetic reconstruction will facilitate efficiency and robust digital evolution simulations at scale, but introduces a complicating factor into phylogenetic analyses: tree reconstruction error. A clear understanding of the impact of these errors on the computed phylometrics will be necessary for informative future phylogenetic analyses.

To explore this question, we compared phylometrics computed on reconstructed trees to corresponding true reference trees under the simple model (Wilcoxon tests; $n = 50$ per condition; Supplementary Table ??). To err towards conservatism in detecting phylometric biases, we did not correct for multiple comparisons. Reconstructions were performed across a range of precisions, ranging from 1% relative resolution for MRCA estimates (most precise) to 33% relative resolution for MRCA estimates (least precise). Precision was manipulated by adjusting the information content of underlying hereditary stratigraphic genome annotations used to perform phylogenetic reconstruction (Moreno et al., 2022a). Note that important differences exist the between nature of reconstruction error under hereditary stratigraphy versus traditional biosequence-based methods, discussed further below.

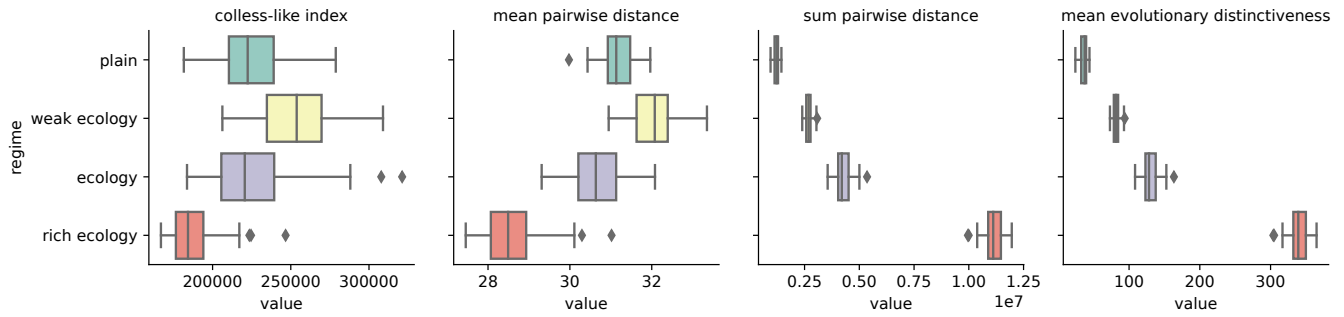
Phylometric Sensitivity to Reconstruction Error

For each phylometric, we sought to determine the minimum resolution required to achieve statistical non-detection (i.e., $p > 0.05$) of bias between reconstructions and their corresponding references. For nearly all cases, 3% reconstruction resolution was sufficient to achieve statistical indistinguishability between reference and reconstruction. Mean evolutionary distinctiveness and sum pairwise distance were particularly robust to reconstruction error, showing no detectable bias even at only 33% reconstruction resolution.

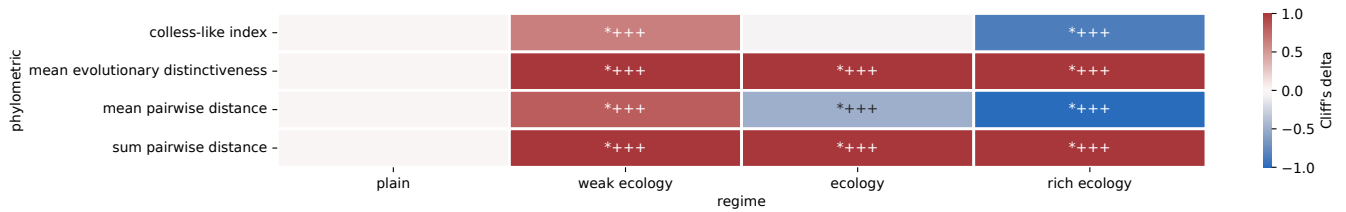
Phylometric sensitivity to reconstruction error was broadly consistent across evolutionary regimes. Figure 10 summarizes these results.

Where detectable, estimation uncertainty bias decreased all surveyed phylometrics' numerical value. So, when testing for expected increases in phylometric values, the potential for systematic false positives due to reconstruction error can be discounted. Supplementary Figure ?? provides a full comparison of the distribution of phylometric estimates on reference trees with the distributions of phylometric estimates for reconstructed trees across reconstruction resolutions.

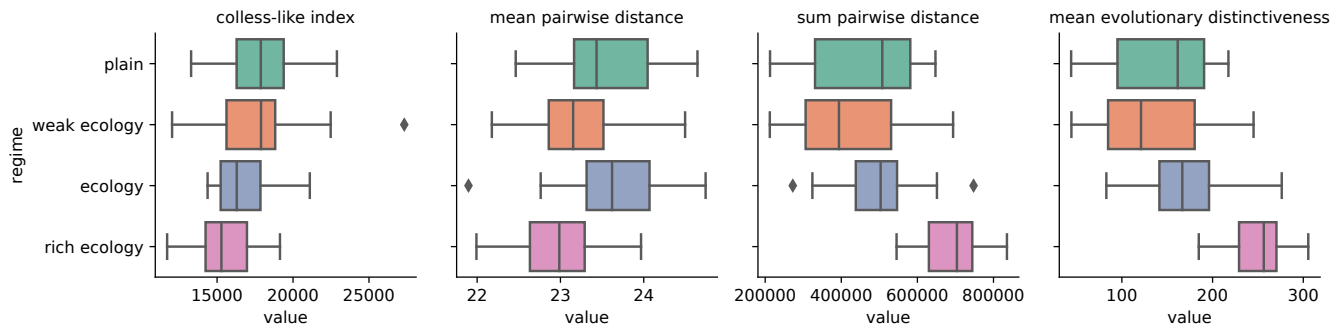
The relationship between reconstruction error and phylometric bias was similar under spatially structured regimes, the alternate exponential mutation operator, at earlier phylogeny sampling time



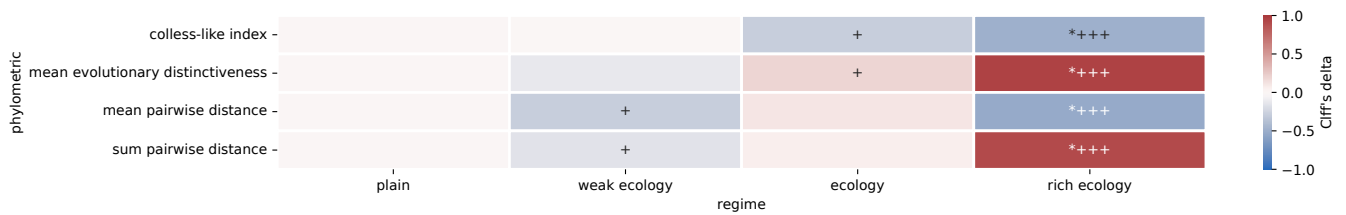
(a) Distribution of phylometrics under the simple model. Sample sizes $n = 50$.



(b) Sizes of the effect of evolutionary regimes on each phylometric relative to “plain” baseline in the simple model. Sample sizes $n = 50$.



(c) Distribution of phylometrics in Avida. Sample sizes $n = 30$.



(d) Sizes of the effect of evolutionary regimes on each phylometric relative to “plain” baseline in Avida. Sample sizes $n = 30$.

Figure 7: Phylometric responses under spatial structure. Distribution of phylometrics across the three surveyed ecological regimes and the control non-ecological regime—all with spatial population structure (i.e., island count 1,024 for simple model, toroidal population grid for Avida). Phylometrics were calculated on perfect-fidelity phylogenies. Note that nonparametric effect size normalization caps out to 1.0/-1.0 past the point of complete disributional nonoverlap. For heatmap charts, +’s indicate small, medium, and large effect sizes using the Cliff’s delta statistic and *’s indicate statistical significance at $\alpha = 0.05$ via Mann-Whitney U test. Results from simple model are for standard experimental conditions: gaussian mutation distribution at epoch 7 (generation 262,144). See Figure ?? for results under sensitivity analysis conditions.

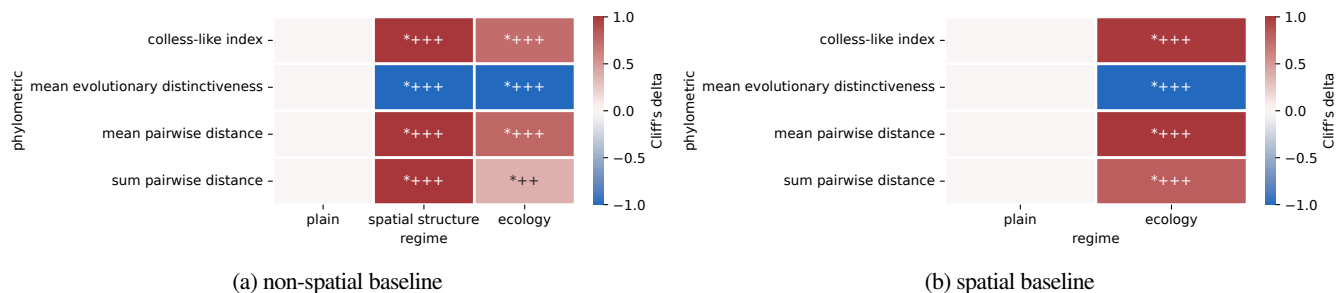


Figure 8: Evolutionary regimes' effect sizes relative to “plain” baseline under the Gen3sis model with perfect phylogenetic tracking, normalized via Cliff's delta. Sample sizes $n = 30$. Annotated +'s indicate small, medium, and large effect sizes using the Cliff's delta statistic and *'s indicate statistical significance at $\alpha = 0.05$ via Mann-Whitney U test.

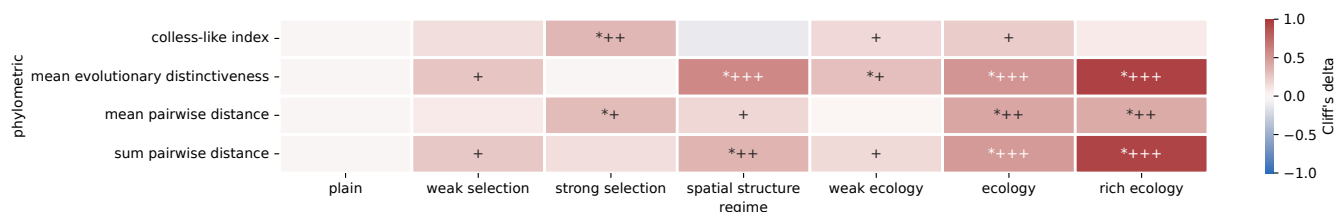


Figure 9: **Phylometrics for genotype-level phylogenies in Avida.** Tree phylometrics across surveyed evolutionary regimes, calculated on perfect-fidelity simulation phylogenies in which the taxonomic unit is genotype rather than individual. Note that nonparametric effect size normalization caps out to 1.0/-1.0 past the point of complete disributional nonoverlap. For heatmap charts, +'s indicate small, medium, and large effect sizes using the Cliff's delta statistic and *'s indicate statistical significance at $\alpha = 0.05$ via Mann-Whitney U test.

points, and in the Avida model system (Supplementary Figures ?????????; Supplementary Table ???). Notably, however, reconstruction bias persisted at even 1% relative resolution in some conditions of the sensitivity analysis and Avida experiments. Forthcoming work has found that the byte-differentia hereditary stratigraphy configuration used for this experiment tends to lump closely contemporaneous lineage splitting events into a polytomy rather than a double-branching event — i.e., indicating uncertainty rather than introducing error. In contrast, reconstructions on single-bit differentia contain erroneously- sequenced branching rather than artifactual polytomies. So, future work should explore whether working with single bit differentia could lessen phylometric bias.

Detection of Evolutionary Drivers' Signatures in Reconstructed Phylogenies

Our last objective was to assess how reconstruction error might affect detection of phylometric signatures induced by treatment conditions. That is, we sought to perform a sort of “integration test” for detection of treatment conditions when working with imperfect reconstructions rather than perfect phylogenies. To this end, we compared the phylometric outcomes of strong/weak selection, spatial structure, ecology, and weak/rich ecology relative to plain conditions for phylogenies reconstructed at 1%, 3%, 10%, and 33% resolution levels. Supplemental Figures ??? show heatmaps with sign, effect size, and significance of phylometric effects across gradations of reconstruction precision for the simple model and Avida, respectively. In most cases, 3% resolution sufficed to fully recover phylometric effects of treatments observed with perfectly-tracked phylogenies.

Conclusion

Because phylogenies are an abstraction that generalizes across all evolutionary processes, phylogenetic analysis can be applied across a breadth of biological and artificial life systems. Consequently, a broad set of cross-disciplinary use cases exist for inferring the processes that shaped a phylogeny by quantifying its topology. Indeed, extraction of information about evolutionary dynamics from phylogenetic history has been a longstanding and productive theme in evolutionary biology (Pagel, 1997). This work seeks to contribute in that vein, by establishing foundations necessary to assess three fundamental evolutionary drivers — spatial structure, ecology, and selection pressure — in complex, distributed evolving populations.

First, we investigated the strength and character of structural signatures in phylogenetic histories left by selection pressure, ecology, and spatial population structure. These drivers induced readily detectable effects across our suite of four surveyed phylometrics. These effects were generally consistent across surveyed individual-level phylogenies, but differed notably under genotype-level tracking and under species-level simulation. Although the directions of phylometric effects were generally consistent across treatments expected to increase phylogenetic richness (i.e., weak selection, ecologies, and spatial structure), effect significance/size for particular phylometrics differed among some treatments. Compared to results from the simple model, which was amenable to strong treatment manipulations, the more sophisticated Avida model system expressed fewer phylometric effects between treatments.

Compared to spatial structure and selection pressure, drivers designed to induce ecological coexistence exerted relatively

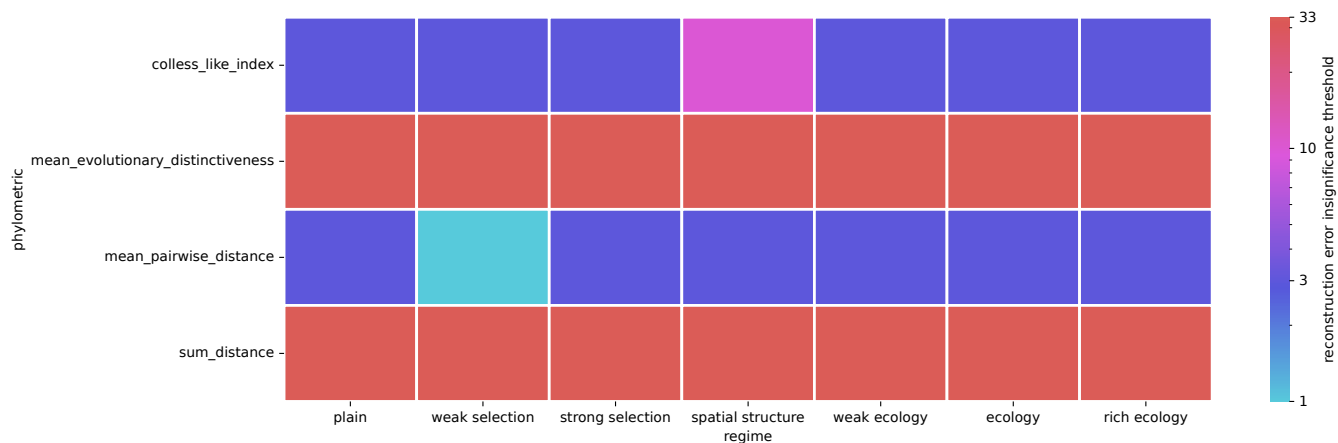


Figure 10: **Reconstruction resolutions required to achieve statistical indistinguishability between reconstructions and ground-truth reference trees.** Significance level $p < 0.05$ under the Wilcoxon signed-rank test between samples of 50 replicates each is used as the threshold for statistical distinguishability. Phylometrics with looser reconstruction resolution thresholds (i.e., higher resolution percentages) are less sensitive to reconstruction error. White heat map tiles indicate that no surveyed reconstruction resolution threshold was sufficient to achieve indistinguishability from the reference tree with respect a particular phylometric. See Supplementary Figure ?? for sensitivity analysis results.

mutated, sparse effects on phylogenetic metrics. However, follow-up experiments with both individual-level model systems revealed that phylometric signatures can remain detectable under background conditions of spatial population structure. Interactions, though, are sometimes surprising. A notable example is the reduced mean pairwise distance observed in *Avida* under conditions combining spatial structure and ecology, but not in the baseline ecology treatment. These results highlight the complexity of how interacting evolutionary dynamics impact phylogenetic structure. Even a single dynamic in isolation can influence phylometrics in opposite directions. For instance, we found that changes to selection pressure in either direction significantly reduced trees' Colless-like index under the simple model.

Comparison of phylometrics from perfect-fidelity trees against corresponding reconstructions revealed that phylometric statistics differed in sensitivity to reconstruction error introduced by hereditary stratigraphy-based tracking. Colless-like index and mean pairwise distance were more sensitive, and in some conditions, reconstruction persisted at even 1% reconstruction resolution. On the other hand, mean evolutionary distinctiveness and sum pairwise distance were particularly robust to reconstruction error, with no bias detected even at 33% reconstruction. Results suggest 3% reconstruction resolution as a reasonable ballpark parameterization for applications of hereditary stratigraphy with downstream phylogenetic analysis. Where it did occur, the sign effect of phylometric bias was consistent, which might simplify considerations to account for it in experiments.

Our findings identify key next steps necessary for development of rigorous phylogenetic assays to test for key evolutionary drivers. Because treatments did not induce widespread opposite-sign effects, our results do not indicate a straightforward, qualitative approach to disambiguate drivers' signatures. Future work should survey comprehensive panels of phylometrics, which might provide a stronger foothold to this end (Tucker et al., 2017).

Alternately, more sophisticated quantitative approaches leveraging differential effect size ratios may be fruitful. Possibilities include application of machine learning techniques over broad phylometric panels (Voznica et al., 2022) or even inference directly over phylogenetic structure itself via graph neural networks and related methods (Lajaaity et al., 2023). The capability of artificial life approaches to generate high-quality data sets with high replication counts will be a significant asset to such work. More information could be harnessed by incorporating trait data (Nozoe et al., 2017) or by using time-sampled phylogenies (Volz et al., 2013), which would include information about "ghost" lineages that have extincted at earlier time points.

Additionally, robust normalization methods will be crucial to enable meaningful comparisons between phylogenies differing in (1) population size, (2) population subsampling level, (3) depth of evolutionary history, and (4) demographic characteristics of organism life histories. Despite some substantial work on this front (Shao & Sokal, 1990; Mir et al., 2018a), significant challenges remain. It is worth noting that most analysis reported here normalizes to phylometric values sampled from "plain" evolutionary regimes, thereby implicitly depending on the availability of such data. However, stripped-down baseline condition experiments may not always be possible, especially in biological model systems. Extensive, likely sophisticated, considerations would be necessary to establish *a priori* phylometric value predictions that could be compared against instead of testing against empirical values. Finally, as evidenced in our experiments, reconstruction error can systematically bias phylometric values. In scenarios where reconstruction error is unavoidable, additional normalizations may be necessary. However, it is promising that some phylometrics appear thoroughly robust to reconstruction error and, in other cases, sufficient reconstruction accuracy might be achieved to obviate error bias.

The overriding objective of work presented here is to equip biologists and computational researchers with capability to

investigate fundamental evolutionary drivers within large-scale evolving populations. To this end, methodology must advance hand-in-hand with the software infrastructure required to put it into practice. Artificial life experiments, specifically, tend to require particular instrumentation to collect phylogenetic histories, and we have been active in making general-use plug-and-play solutions available freely through the Python Packaging Index (Moreno et al., 2022b; Dolson et al., 2024). As each field develops, artificial life will benefit greatly from domain-specific software and methods developed within traditional evolutionary bioinformatics and, vice versa.

Acknowledgment

This research was supported in part by NSF grants DEB-1655715 and DBI-0939454 as well as by Michigan State University through the computational resources provided by the Institute for Cyber-Enabled Research. This material is based upon work supported by the National Science Foundation Graduate Research Fellowship under Grant No. DGE-1424871. Any opinions, findings, and conclusions or recommendations expressed in this material are those of the author(s) and do not necessarily reflect the views of the National Science Foundation. This material is based upon work supported by the Eric and Wendy Schmidt AI in Science Postdoctoral Fellowship, a Schmidt Futures program.

References

- Ackley, D. & Small, T. (2014). Indefinitely scalable computing=artificial life engineering. *ALIFE 14: The Fourteenth International Conference on the Synthesis and Simulation of Living Systems*, 606–613.
- Adami, C. (2006). Digital genetics: unravelling the genetic basis of evolution. *Nature Reviews Genetics*, 7(2), 109–118.
- Annan, J. & Hargreaves, J. C. (2013). A new global reconstruction of temperature changes at the last glacial maximum. *Climate of the Past*, 9(1), 367–376.
- Arbogast, B. S., Edwards, S. V., Wakeley, J., Beerli, P., & Slowinski, J. B. (2002). Estimating divergence times from molecular data on phylogenetic and population genetic timescales. *Annual review of Ecology and Systematics*, 33(1), 707–740.
- Blomberg, A. (2011). Measuring growth rate in high-throughput growth phenotyping. *Current opinion in biotechnology*, 22(1), 94–102.
- Burke, E. K., Gustafson, S., Kendall, G., & Krasnogor, N. (2003). Is increased diversity in genetic programming beneficial? an analysis of lineage selection. *The 2003 Congress on Evolutionary Computation, 2003. CEC'03.*, volume 2, 1398–1405.
- Burrell, E. D. & Tan, M. (2017). Ecological opportunity alters the timing and shape of adaptive radiation. *Evolution*, n/a–n/a. <https://doi.org/10.1111/evo.13362>
- Chamberlain, S., Vázquez, D. P., Carvalheiro, L., Elle, E., & Vamosi, J. C. (2014). Phylogenetic tree shape and the structure of mutualistic networks. *Journal of Ecology*, 102(5), 1234–1243. <https://doi.org/10.1111/1365-2745.12293>
- Cliff, N. (1993). Dominance statistics: Ordinal analyses to answer ordinal questions. *Psychological bulletin*, 114(3), 494.
- Cock, P. J., Antao, T., Chang, J. T., Chapman, B. A., Cox, C. J., Dalke, A., Friedberg, I., Hamelryck, T., Kauff, F., Wilczynski, B., et al. (2009). Biopython: freely available python tools for computational molecular biology and bioinformatics. *Bioinformatics*, 25(11), 1422–1423.
- Colless, D. H. (1982). Review of phylogenetics: The theory and practice of phylogenetic systematics. *Systematic Zoology*, 31(1), 100–104. <https://doi.org/10.2307/2413420>. Publisher: [Oxford University Press, Society of Systematic Biologists, Taylor & Francis, Ltd.]
- Cramwinckel, M. J., Huber, M., Kocken, I. J., Agnini, C., Bijl, P. K., Bohaty, S. M., Frieling, J., Goldner, A., Hilgen, F. J., Kip, E. L., et al. (2018). Synchronous tropical and polar temperature evolution in the eocene. *Nature*, 559(7714), 382–386.
- Dolson, E., Lalejini, A., Jorgensen, S., & Ofria, C. (2020). Interpreting the tape of life: ancestry-based analyses provide insights and intuition about evolutionary dynamics. *Artificial Life*, 26(1), 58–79.
- Dolson, E., Moreno, M. A., & rodsan0 (2024). *emilydolson/phylotrackpy: v0.2.0*. <https://doi.org/10.5281/zenodo.10888780>
- Dolson, E. L., Vostinar, A. E., Wisner, M. J., & Ofria, C. (2019). The MODES toolbox: Measurements of open-ended dynamics in evolving systems. *Artificial Life*, 25(1), 50–73. https://doi.org/10.1162/artl_a_00280
- Evans, D., Sagoo, N., Renema, W., Cotton, L. J., Müller, W., Todd, J. A., Saraswati, P. K., Stassen, P., Ziegler, M., Pearson, P. N., et al. (2018). Eocene greenhouse climate revealed by coupled clumped isotope-mg/ca thermometry. *Proceedings of the National Academy of Sciences*, 115(6), 1174–1179.
- Ferguson, A. J. & Ofria, C. (2023). Potentiating mutations facilitate the evolution of associative learning in digital organisms. *ALIFE 2023: Ghost in the Machine: Proceedings of the 2023 Artificial Life Conference*.
- Fick, S. E. & Hijmans, R. J. (2017). Worldclim 2: new 1-km spatial resolution climate surfaces for global land areas. *International journal of climatology*, 37(12), 4302–4315.
- Forest, F., Grenyer, R., Rouget, M., Davies, T. J., Cowling, R. M., Faith, D. P., Balmford, A., Manning, J. C., Proches, S., van der Bank, M., Reeves, G., Hedderson, T. A. J., & Savolainen, V. (2007). Preserving the evolutionary potential of floras in biodiversity hotspots. *Nature*, 445(7129), 757–760. <https://doi.org/10.1038/nature05587>

- Foster, E. D. & Deardorff, A. (2017). Open science framework (osf). *Journal of the Medical Library Association: JMLA*, 105(2), 203.
- Giardina, F., Romero-Severson, E. O., Albert, J., Britton, T., & Leitner, T. (2017). Inference of transmission network structure from hiv phylogenetic trees. *PLoS computational biology*, 13(1), e1005316.
- Hagen, O., Flück, B., Fopp, F., Cabral, J. S., Hartig, F., Pontarp, M., Rangel, T. F., & Pellissier, L. (2021). gen3sis: A general engine for eco-evolutionary simulations of the processes that shape earth's biodiversity. *PLoS Biology*, 19(7), e3001340.
- Hagen, O., Vaterlaus, L., Albouy, C., Brown, A., Leugger, F., Onstein, R. E., de Santana, C. N., Scotese, C. R., & Pellissier, L. (2019). Mountain building, climate cooling and the richness of cold-adapted plants in the northern hemisphere. *Journal of Biogeography*, 46(8), 1792–1807.
- Harris, C. R., Millman, K. J., van der Walt, S. J., Gommers, R., Virtanen, P., Cournapeau, D., Wieser, E., Taylor, J., Berg, S., Smith, N. J., Kern, R., Picus, M., Hoyer, S., van Kerkwijk, M. H., Brett, M., Haldane, A., del Río, J. F., Wiebe, M., Peterson, P., Gérard-Marchant, P., Sheppard, K., Reddy, T., Weckesser, W., Abbasi, H., Gohlke, C., & Oliphant, T. E. (2020). Array programming with NumPy. *Nature*, 585(7825), 357–362. <https://doi.org/10.1038/s41586-020-2649-2>
- Hernandez, J. G., Lalejini, A., & Dolson, E. (2022). What can phylogenetic metrics tell us about useful diversity in evolutionary algorithms? *Genetic Programming Theory and Practice XVIII*, Genetic and Evolutionary Computation, 63–82. Springer Nature. https://doi.org/10.1007/978-981-16-8113-4_4
- Hess, M. R. & Kromrey, J. D. (2004). Robust confidence intervals for effect sizes: A comparative study of cohen's d and cliff's delta under non-normality and heterogeneous variances. *annual meeting of the American Educational Research Association*, volume 1.
- Hindré, T., Knibbe, C., Beslon, G., & Schneider, D. (2012). New insights into bacterial adaptation through in vivo and in silico experimental evolution. *Nature Reviews Microbiology*, 10(5), 352–365.
- Hollis, C. J., Dunkley Jones, T., Anagnostou, E., Bijl, P. K., Cramwinckel, M. J., Cui, Y., Dickens, G. R., Edgar, K. M., Eley, Y., Evans, D., et al. (2019). The deepmip contribution to pmip4: Methodologies for selection, compilation and analysis of latest paleocene and early eocene climate proxy data, incorporating version 0.1 of the deepmip database. *Geoscientific Model Development*, 12(7), 3149–3206.
- Hunter, J. D. (2007). Matplotlib: A 2d graphics environment. *Computing in Science & Engineering*, 9(3), 90–95. <https://doi.org/10.1109/mcse.2007.55>
- Hutchinson, D. K., de Boer, A. M., Coxall, H. K., Caballero, R., Nilsson, J., & Baatsen, M. (2018). Climate sensitivity and meridional overturning circulation in the late eocene using gfdl cm2. 1. *Climate of the Past*, 14(6), 789–810.
- Isaac, N. J. B., Turvey, S. T., Collen, B., Waterman, C., & Baillie, J. E. M. (2007). Mammals on the EDGE: Conservation priorities based on threat and phylogeny. *Plos One*, 2(3), e296. <https://doi.org/10.1371/journal.pone.0000296>
- Izsák, J. & Papp, L. (2000). A link between ecological diversity indices and measures of biodiversity. *Ecological Modelling*, 130(1), 151–156. [https://doi.org/10.1016/S0304-3800\(00\)00203-9](https://doi.org/10.1016/S0304-3800(00)00203-9)
- James, T. Y., Kauff, F., Schoch, C. L., Matheny, P. B., Hofstetter, V., Cox, C. J., Celio, G., Gueidan, C., Fraker, E., Miadlikowska, J., et al. (2006). Reconstructing the early evolution of fungi using a six-gene phylogeny. *Nature*, 443(7113), 818–822.
- Johnson, K., Welch, P., Dolson, E., & Vostinar, A. E. (2022). Endosymbiosis or bust: Influence of eotymbiosis on evolution of obligate endosymbiosis. *ALIFE 2022: The 2022 Conference on Artificial Life*. https://doi.org/10.1162/isal_a_00488
- Kane Meissel, E. S. Y. (2024). Using cliff's delta as a non-parametric effect size measure: An accessible web app and tutorial. *Practical Assessment, Research, and Evaluation*, 29. <https://doi.org/10.7275/pare.1977>
- Keating-Bitonti, C. R., Ivany, L. C., Affek, H. P., Douglas, P., & Samson, S. D. (2011). Warm, not super-hot, temperatures in the early eocene subtropics. *Geology*, 39(8), 771–774.
- Klasky, S., Thayer, J., & Najm, H. (2021). Data reduction for science: Brochure from the advanced scientific computing research workshop. Technical report, Oak Ridge National Lab.(ORNL), Oak Ridge, TN (United States); SLAC National ...
- Kojima, H. & Ikegami, T. (2023). Implementation of lenia as a reaction-diffusion system. *ALIFE 2023: Ghost in the Machine: Proceedings of the 2023 Artificial Life Conference*.
- Lajaaity, I., Lambert, S., Voznica, J., Morlon, H., & Hartig, F. (2023). A comparison of deep learning architectures for inferring parameters of diversification models from extant phylogenies. *bioRxiv*, 2023–03.
- Lalejini, A., Dolson, E., Bohm, C., Ferguson, A. J., Parsons, D. P., Rainford, P. F., Richmond, P., & Ofria, C. (2019). Data standards for artificial life software. *ALIFE 2019: The 2019 Conference on Artificial Life*, 507–514.
- Lalejini, A., Moreno, M. A., Hernandez, J. G., & Dolson, E. (2024). Phylogeny-informed fitness estimation for test-based parent selection. *Genetic Programming Theory and Practice XX*, 241–261. Springer International Publishing. https://doi.org/10.1007/978-981-99-8413-8_13

- Lalejini, A. & Ofria, C. (2016). The evolutionary origins of phenotypic plasticity. *Proceedings of the Artificial Life Conference 2016*, 372–379. <https://doi.org/10.7551/978-0-262-33936-0-ch063>
- Lenski, R. E., Ofria, C., Pennock, R. T., & Adami, C. (2003). The evolutionary origin of complex features. *Nature*, 423(6936), 139–144. <https://doi.org/10.1038/nature01568>
- Lewinsohn, M. A., Bedford, T., Müller, N. F., & Feder, A. F. (2023). State-dependent evolutionary models reveal modes of solid tumour growth. *Nature Ecology & Evolution*, 1–16. <https://doi.org/10.1038/s41559-023-02000-4>. Publisher: Nature Publishing Group
- Mann, H. B. & Whitney, D. R. (1947). On a test of whether one of two random variables is stochastically larger than the other. *The Annals of Mathematical Statistics*, 18(1), 50 – 60. <https://doi.org/10.1214/aoms/1177730491>
- Mir, A., Rotger, L., & Rosselló, F. (2018a). Sound colless-like balance indices for multifurcating trees. *PLoS one*, 13(9), e0203401.
- Mir, A., Rotger, L., & Rosselló, F. (2018b). Sound colless-like balance indices for multifurcating trees. *Plos One*, 13(9), e0203401. <https://doi.org/10.1371/journal.pone.0203401>. Publisher: Public Library of Science
- Moreno, M. A. (2023). *mmore500/teeplot*. <https://doi.org/10.5281/zenodo.10440670>
- Moreno, M. A. (2024a). Methods for rich phylogenetic inference over distributed sexual populations. *Genetic Programming Theory and Practice XX*, 125–141. Springer International Publishing. https://doi.org/10.1007/978-981-99-8413-8_7
- Moreno, M. A. (2024b). *mmore500/qspool*. <https://doi.org/10.5281/zenodo.10864602>
- Moreno, M. A., Dolson, E., & Ofria, C. (2022a). Hereditary stratigraphy: Genome annotations to enable phylogenetic inference over distributed populations. *ALIFE 2022: The 2022 Conference on Artificial Life*, volume 7, 4866. https://doi.org/10.1162/isal_a_00550
- Moreno, M. A., Dolson, E., & Ofria, C. (2022b). hstrat: a python package for phylogenetic inference on distributed digital evolution populations. *Journal of Open Source Software*, 7(80), 4866. <https://doi.org/10.21105/joss.04866>
- Moreno, M. A., Dolson, E., & Rodriguez-Papa, S. (2023). Toward phylogenetic inference of evolutionary dynamics at scale. *ALIFE 2023: Ghost in the Machine: Proceedings of the 2023 Artificial Life Conference*, ALIFE 2023: Ghost in the Machine: Proceedings of the 2023 Artificial Life Conference, 79. https://doi.org/10.1162/isal_a_00694
- Moreno, M. A. & Ofria, C. (2022). Exploring evolved multicellular life histories in an open-ended digital evolution system. *Frontiers in Ecology and Evolution*, 10. <https://doi.org/10.3389/fevo.2022.750837>
- Moreno, M. A. & Papa, S. R. (2024). *mmore500/alifedata-phyloinformatics-convert*. <https://doi.org/10.5281/zenodo.10701178>
- Moreno, M. A., Papa, S. R., & Dolson, E. (2024). *Analysis of phylogeny tracking algorithms for serial and multiprocess applications*. <https://doi.org/10.48550/arXiv.2403.00246>
- Moreno, M. A., Rodriguez Papa, S., & Ofria, C. (2021). Conduit: A c++ library for best-effort high performance computing. *Proceedings of the Genetic and Evolutionary Computation Conference Companion, Gecco '21*, 1795–1800. <https://doi.org/10.1145/3449726.3463205>
- Nozoe, T., Kussell, E., & Wakamoto, Y. (2017). Inferring fitness landscapes and selection on phenotypic states from single-cell genealogical data. *PLoS genetics*, 13(3), e1006653.
- Ofria, C., Moreno, M. A., Dolson, E., Lalejini, A., Rodriguez Papa, S., Fenton, J., Perry, K., Jorgensen, S., hoffmanriley, grenewode, Baldwin Edwards, O., Stredwick, J., cgnitash, theycallmeHeem, Vostinar, A., Moreno, R., Schossau, J., Zaman, L., & djrain (2020). Empirical: C++ library for efficient, reliable, and accessible scientific software. *Zenodo*. <https://doi.org/10.5281/zenodo.4141943>
- Ofria, C. & Wilke, C. O. (2004). Avida: A software platform for research in computational evolutionary biology. *Artificial life*, 10(2), 191–229.
- Pagel, M. (1997). Inferring evolutionary processes from phylogenies. *Zoologica Scripta*, 26(4), 331–348.
- Pagel, M. (1999). Inferring the historical patterns of biological evolution. *Nature*, 401(6756), 877–884.
- pandas development team, T. (2020). pandas-dev/pandas: Pandas. *Zenodo*. <https://doi.org/10.5281/zenodo.3509134>
- Rabosky, D. L. & Lovette, I. J. (2008). Density-dependent diversification in north american wood warblers. *Proceedings of the Royal Society B: Biological Sciences*, 275(1649), 2363–2371.
- Sand, A., Holt, M. K., Johansen, J., Brodal, G. S., Mailund, T., & Pedersen, C. N. (2014). tqdist: a library for computing the quartet and triplet distances between binary or general trees. *Bioinformatics*, 30(14), 2079–2080.
- Saulnier, E., Gascuel, O., & Alizon, S. (2017). Inferring epidemiological parameters from phylogenies using regression-abc: A comparative study. *PLoS computational biology*, 13(3), e1005416.

- Schneider, S., Taylor, G. W., Linquist, S., & Kremer, S. C. (2019). Past, present and future approaches using computer vision for animal re-identification from camera trap data. *Methods in Ecology and Evolution*, 10(4), 461–470.
- Scott, J. G., Maini, P. K., Anderson, A. R. A., & Fletcher, A. G. (2020). Inferring tumor proliferative organization from phylogenetic tree measures in a computational model. *Systematic Biology*, 69(4), 623–637. <https://doi.org/10/gmxwzq>
- Shahbandegan, S., Hernandez, J. G., Lalejini, A., & Dolson, E. (2022). Untangling phylogenetic diversity's role in evolutionary computation using a suite of diagnostic fitness landscapes. *Proceedings of the Genetic and Evolutionary Computation Conference Companion, Gecco '22*, 2322–2325. <https://doi.org/10.1145/3520304.3534028>
- Shao, K.-T. (1990). Tree balance. *Systematic Biology*, 39(3), 266–276. <https://doi.org/10.2307/2992186>
- Shao, K.-T. & Sokal, R. R. (1990). Tree balance. *Systematic Zoology*, 39(3), 266–276.
- Sijp, W. P., von der Heydt, A. S., Dijkstra, H. A., Flögel, S., Douglas, P. M., & Bijl, P. K. (2014). The role of ocean gateways on cooling climate on long time scales. *Global and Planetary Change*, 119, 1–22.
- Straume, E. O., Gaina, C., Medvedev, S., & Nisancioglu, K. H. (2020). Global cenozoic paleobathymetry with a focus on the northern hemisphere oceanic gateways. *Gondwana Research*, 86, 126–143.
- Sukumaran, J. & Holder, M. T. (2010). Dendropy: a python library for phylogenetic computing. *Bioinformatics*, 26(12), 1569–1571.
- Torchiano, M. (2016). *Effsize - a package for efficient effect size computation*. <https://doi.org/10.5281/zenodo.196082>
- Tucker, C. M., Cadotte, M. W., Carvalho, S. B., Davies, T. J., Ferrier, S., Fritz, S. A., Grenyer, R., Helmus, M. R., Jin, L. S., Mooers, A. O., Pavoine, S., Purschke, O., Redding, D. W., Rosauer, D. F., Winter, M., & Mazel, F. (2017). A guide to phylogenetic metrics for conservation, community ecology and macroecology. *Biological Reviews*, 92(2), 698–715. <https://doi.org/10.1111/brv.12252>
- Virtanen, P., Gommers, R., Oliphant, T. E., Haberland, M., Reddy, T., Cournapeau, D., Burovski, E., Peterson, P., Weckesser, W., Bright, J., van der Walt, S. J., Brett, M., Wilson, J., Millman, K. J., Mayorov, N., Nelson, A. R. J., Jones, E., Kern, R., Larson, E., Carey, C. J., Polat, İ., Feng, Y., Moore, E. W., VanderPlas, J., Laxalde, D., Perktold, J., Cimrman, R., Henriksen, I., Quintero, E. A., Harris, C. R., Archibald, A. M., Ribeiro, A. H., Pedregosa, F., van Mulbregt, P., & SciPy 1.0 Contributors (2020). SciPy 1.0: Fundamental Algorithms for Scientific Computing in Python. *Nature Methods*, 17, 261–272. <https://doi.org/10.1038/s41592-019-0686-2>
- Volz, E. M., Koelle, K., & Bedford, T. (2013). Viral phylogenomics. *PLoS computational biology*, 9(3), e1002947.
- Voznica, J., Zhukova, A., Boskova, V., Saulnier, E., Lemoine, F., Moslonka-Lefebvre, M., & Gascuel, O. (2022). Deep learning from phylogenies to uncover the epidemiological dynamics of outbreaks. *Nature Communications*, 13(1), 3896.
- Waskom, M. L. (2021). seaborn: statistical data visualization. *Journal of Open Source Software*, 6(60), 3021. <https://doi.org/10.21105/joss.03021>
- Webb, C. O. & Losos, A. E. J. B. (2000). Exploring the phylogenetic structure of ecological communities: An example for rain forest trees. *The American Naturalist*, 156(2), 145–155. <https://doi.org/10.1086/303378>
- Wes McKinney (2010). Data Structures for Statistical Computing in Python. *Proceedings of the 9th Python in Science Conference*, 56–61. <https://doi.org/10.25080/Majora-92bf1922-00a>
- Westerhold, T., Marwan, N., Drury, A. J., Liebrand, D., Agnini, C., Anagnostou, E., Barnet, J. S., Bohaty, S. M., De Vleeschouwer, D., Florindo, F., et al. (2020). An astronomically dated record of earth's climate and its predictability over the last 66 million years. *Science*, 369(6509), 1383–1387.
- Woodworth, M. B., Girskis, K. M., & Walsh, C. A. (2017). Building a lineage from single cells: genetic techniques for cell lineage tracking. *Nature Reviews Genetics*, 18(4), 230–244.
- Zhang, L., Hay, W. W., Wang, C., & Gu, X. (2019). The evolution of latitudinal temperature gradients from the latest cretaceous through the present. *Earth-Science Reviews*, 189, 147–158.